

Dalton Transactions

Accepted Manuscript



This is an *Accepted Manuscript*, which has been through the Royal Society of Chemistry peer review process and has been accepted for publication.

Accepted Manuscripts are published online shortly after acceptance, before technical editing, formatting and proof reading. Using this free service, authors can make their results available to the community, in citable form, before we publish the edited article. We will replace this *Accepted Manuscript* with the edited and formatted *Advance Article* as soon as it is available.

You can find more information about *Accepted Manuscripts* in the [Information for Authors](#).

Please note that technical editing may introduce minor changes to the text and/or graphics, which may alter content. The journal's standard [Terms & Conditions](#) and the [Ethical guidelines](#) still apply. In no event shall the Royal Society of Chemistry be held responsible for any errors or omissions in this *Accepted Manuscript* or any consequences arising from the use of any information it contains.

ARTICLE

Architectural control of urea in supramolecular 1D strontium vanadium oxide chains

Cite this: DOI: 10.1039/x0xx00000x

Benjamin Schwarz^a and Carsten Streb^aReceived 00th January 2012,
Accepted 00th January 2012

DOI: 10.1039/x0xx00000x

www.rsc.org/

A facile bottom-up approach for the controlled self-assembly of infinite strontium vanadium oxide chains is presented. Two novel one-dimensional strontium-linked polyoxovanadate chains have been isolated by linkage of decavanadate clusters with strontium(II) ions. To control the architecture dimensions, urea was used as a critical control parameter which allowed tuning of the intra- and intermolecular spacings within the crystal lattice. Using *N,N*-dimethyl formamide (DMF) and urea as stabilizing ligands, a supramolecular structure, $\{[\text{Sr}(\text{dmf})_3(\text{CON}_2\text{H}_4)_2][\text{Sr}(\text{dmf})_2(\text{CON}_2\text{H}_4)_2][\text{H}_2\text{V}_{10}\text{O}_{28}]\}$ (**1**) was obtained where cluster linkage is achieved through urea-bridged strontium dimers. In the absence of urea, a purely strontium-linked supramolecular architecture, $\{[\text{Sr}(\text{dmf})_4]_2[\text{H}_2\text{V}_{10}\text{O}_{28}]\}$ (**2**), is formed. The chain architectures were characterized by single crystal X-ray diffraction, elemental analysis, UV-Vis and FT-IR spectroscopy. In order to learn about the assembly and dis-assembly of 1D architectures ESI-mass-spectrometry was performed. The results show how simple organic ligands may be used to engineer the crystal lattice and illustrate that further work is needed to understand the exact mode of action of the urea ligands.

Introduction

POMs and their self-assembly

Polyoxometalates (POMs) are molecular metal oxide aggregates and can be considered as molecular analogues of traditional solid state metal oxides.¹⁻⁴ Typically, POMs consist of early transition metals of group 5 and 6 in high oxidation states, mainly molybdenum, tungsten, vanadium and niobium which form stable terminal metal-oxo bonds.^{1, 2} Small metal oxide precursors $[\text{MO}_x]^{n-}$ with $x = 4 - 7$ undergo oligo-condensation reactions in acidic solution to form supramolecular cluster $[\text{M}_x\text{O}_y]^{m-}$. The resulting structures are stabilized by metal oxygen σ - and π -bonds. Terminal M=O double bonds characteristic for POMs show decreased nucleophilicity, thereby limiting cluster growth.¹ Thus, the assembly of complex architectures through bottom-up self-assembly processes is possible.⁵ Further, the cluster structure can be tuned by controlling secondary reaction parameters such as pH-value, reaction temperature, solvent, redox-agents or counter ions. Incorporation of of heteroelements into the cluster shell can also be used to alter the physical and chemical properties of the clusters,⁶ making the materials interesting candidates for catalysis, molecular electronics, medicine and analytical chemistry.⁷ Assembling POM clusters into functional supramolecular inorganic compounds such as 1D-chains, 2D- grids or 3D-frameworks significantly expands the application horizon of these systems.^{5, 8, 9}

Supramolecular POM architectures

The formation of supramolecular POM-based architectures can be achieved by linkage of well-defined POM clusters (i) by direct metal-induced linkage of clusters via M-O-M bonds, (ii) *via* covalent bonds to organic components, which can polymerize, (iii) *via* covalent binding to multitopic organic ligands.¹⁰ Thereby, the linking strategy of choice strongly depends on the type of cluster employed.

A prime example of these concepts was given by ZUBIETA *et al.* who showed that chiral double helices can be formed via self-assembly from simple vanadium oxide precursors.¹¹ Their compound consists of a 3D covalently bonded framework built from vanadium oxo pentamers. The helix repeat unit is formed by four pentamers and two strands of the buildings units are joined to give an inorganic double helix. The helices are held together by phosphate linkages, in similarity to the natural DNA. Further, the structure contains cavities and tunnels and structural analyses show that these voids feature selective binding capabilities for inorganic (e.g. K^+) and organic (e.g. Me_2NH_2^+) cations.

More recently, CRONIN *et al.* showed that supramolecular silver vanadium oxide structures can be in situ converted into composite semiconducting nanostructures.^{12, 13} Linking decavanadate clusters with silver cations, POM-based 1D, and 2D architectures were assembled. Precise reaction control resulted in either silver-terminated 1D chains or in silver-linked 2D networks.

Using a reductive transformation route, both compounds were transformed into extensively cross-connected and interweaved silver-nanoparticle-decorated vanadium oxide nanowires. The composite material was semiconducting, mechanically robust and

could be fashioned into monoliths, demonstrating the technological importance of these materials.

In 2013, inspired by these earlier works, we reported the formation of 1D barium vanadium oxide chains¹³ and giant molecular barium vanadium oxide architectures¹⁴ formed from molecular building blocks by employing coordinating solvents. The decavanadate cluster acts as a ligand to coordinate barium ions as potential coordination sites. The use of the bulky solvents *N,N*-dimethyl formamide (DMF) and *N*-methyl-2-pyrrolidone (NMP) enabled the formation of two chain structures *via* self-assembly. Theoretical analyses showed that the type of solvent ligand employed was critical for the architectures of the chains obtained. To this end, in this report we expand this strategy by investigating the effects of the small, structurally related urea molecule which is employed to study its role as structure directing agent.

Here we present that even a small, sterically non-demanding molecule such as urea can be used to tune the assembly of vanadium oxide chains by enabling specific interactions with the chosen metal ion linkages, here Sr²⁺. We opted to investigate large alkali earth vanadates as their application in solid-state oxidation catalysis (e.g. dehydrogenation) is well known.¹⁵ The use of urea as a potential structure directing was based on chemical considerations regarding their binding ability as well as on literature reports.¹⁶

Results and discussion

Compound 1 – a urea-linked strontium vanadate 1D chain

Compound **1** $\{[\text{Sr}(\text{dmf})_3(\text{CON}_2\text{H}_4)_2][\text{Sr}(\text{dmf})_2(\text{CON}_2\text{H}_4)_2][\text{H}_2\text{V}_{10}\text{O}_{28}]\}$ was synthesized in a one-pot synthesis by the reaction of (ⁿBu₄N)₃[H₃V₁₀O₂₈] (= TBA₃{H₃V₁₀}) with SrBr₂ · 6 H₂O and urea (CON₂H₄) in DMF. Yellow crystalline plates were obtained by diffusion of acetone into the reaction mixture. Structural characterization using single crystal X-ray diffractometry showed that **1** crystallizes in the monoclinic space group *Cc* with cell axes *a* = 10.8044(5) Å, *b* = 23.2995(14) Å, *c* = 22.2340(11) Å, and angles α = 90°, β = 100.681(4)°, γ = 90°, *V* = 5500.1(5) Å³. The crystal lattice of **1** consists of infinite 1D chains, which are based on the archetypal decavanadate cluster anion [H₂V₁₀O₂₈]⁴⁻ (= {V₁₀}) as the principal building block. Linkage between {V₁₀} units is established by two Sr-based bridging units *via* V-O-Sr bonds. Two Sr²⁺ cations coordinate to one terminal oxygen ligand and one adjacent μ -oxo ligand located at the corner of the {V₁₀} unit. One Sr²⁺ ion is found in distorted trigonal prismatic, square face monocapped coordination environment formed by three urea ligands, two DMF molecules and two cluster-based oxo-ligands. The other Sr²⁺ cation is found in distorted square antiprismatic coordination environment formed by three urea ligands, three DMF molecules and two {V₁₀}-based oxo ligands (Fig. 1, top).

Each metal center provides one coordinated urea ligand for the linkage, whereby the carbonyl group acts as a μ^2 -bridge connecting adjacent strontium centers. The terminal ligands are arranged so that the bulky backbone is pointing away from the chain assembly. As a result, an edge-sharing {Sr₂} unit with a Sr-Sr distance of 4.04 Å is formed. It is interesting to note, that the urea ligands align in a co-

parallel fashion. Due to the bridging {Sr₂} dimers, an intermolecular distance between adjacent decavanadate clusters of *ca.* 12.8 Å is observed (Fig. 1, middle). Due to the “off-centered” coordination pattern of strontium centers to {V₁₀} the chain propagates in diagonal manner with respect to the decavanadate building block. In the lattice, the one dimensional chains align in a co-parallel mode within one crystal layer, with opposite directions of chain propagation. Notably, the {V₁₀} cluster units are exclusively surrounded by {Sr₂} bridging units of adjacent chains. Since the bridging unit shows a larger diameter of *ca.* 13 Å compared to *ca.* 10 Å of the {V₁₀} units, this feature could be interpreted as an arrangement with minimum space-requirements. The non-polar moieties of urea and DMF, which point away from the chain assembly, serve as separators between chains. Between chain layers, an inter-layer torsion angle of approximately 130° is observed, see Fig. 1, bottom.

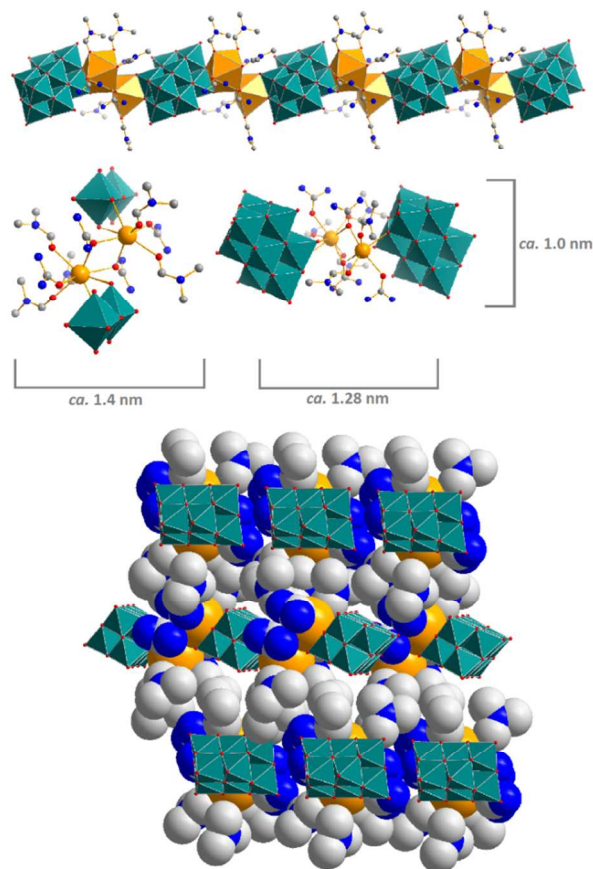


Fig. 1: Illustration of the supramolecular 1D-chain with the corresponding bridging unit observed in **1**. Top: Ball-and-stick and polyhedral representation of the chain showing {V₁₀} units (teal polyhedra) linked by {Sr₂} dimers (orange polyhedra). Center left: {Sr₂} bridging unit $\{[\text{Sr}(\text{dmf})_3(\text{CON}_2\text{H}_4)_2][\text{Sr}(\text{dmf})_2(\text{CON}_2\text{H}_4)_2]\}$; carbonyl groups of urea act as μ^2 -bridge connecting adjacent Sr centers. Notably, the urea ligands align in a parallel fashion. Center right: “Off-centered” coordination pattern of Sr to {V₁₀} units and linkage by urea leads to an inter-cluster distance of *ca.* 1.28 nm. Bottom: Illustration of the crystal packing of **1**. The chains align parallel within on layer. Due to the larger diameter bridging {Sr₂} units are located next to {V₁₀} units of adjacent chains. Between chain layers, an inter-layer torsion angle of approximately 130° is observed. Colour scheme: V: teal, Sr: orange, O: red, N: blue, C: light grey, H atoms are omitted for clarity.

Compound 2 – a DMF-shielded strontium vanadate 1D chain

Compound **2** $\{[\text{Sr}(\text{dmf})_4]_2[\text{H}_2\text{V}_{10}\text{O}_{28}]\}$ was obtained using a similar synthetic route as **1** from a one-pot synthesis of $\text{TBA}_3\{\text{H}_3\text{V}_{10}\}$ and $\text{SrBr}_2 \cdot 6 \text{H}_2\text{O}$ in DMF in the absence of urea. Diffusion of acetone into the reaction mixture resulted in orange crystalline blocks. Structural characterization using single crystal X-ray diffractometry showed that **2** crystallizes in the triclinic space group $P-1$ with cell axes $a = 10.9593(3) \text{ \AA}$, $b = 11.6409(7) \text{ \AA}$, $c = 12.2782(7) \text{ \AA}$, and angles $\alpha = 104.697^\circ$, $\beta = 99.497(4)^\circ$, $\gamma = 109.603(3)^\circ$, $V = 1372.51(13) \text{ \AA}^3$. The compound is virtually isostructural to the barium analogue $\{[\text{Ba}(\text{dmf})_4]_2[\text{H}_2\text{V}_{10}\text{O}_{28}]\}$ reported by us previously.¹³

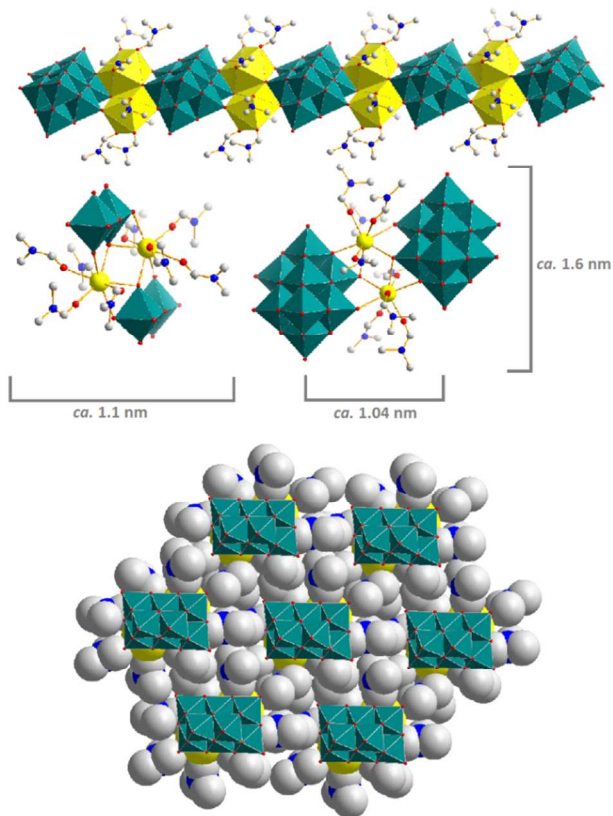


Fig. 2: Illustration of the supramolecular 1D-chain with the corresponding bridging unit observed in **2**. Top: Ball-and-stick and polyhedral representation of the chain structure showing $\{\text{V}_{10}\}$ units (teal polyhedra) linked by $\{\text{Sr}_2\}$ units (yellow polyhedra). Center left: $\{\text{Sr}_2\}$ bridging unit $\{[\text{Sr}(\text{dmf})_4]_2\}$; the Sr centers link directly between adjacent $\{\text{V}_{10}\}$ units. DMF ligands stabilize the bridging unit. Center right: Coordination of Sr^{2+} and direct interaction with adjacent building blocks leads to short inter-cluster distances of *ca.* 1.04 nm. Bottom: Illustration of the crystal packing of **2**. The $\{\text{V}_{10}\}$ units are exclusively surrounded by more bulky $\{\text{Sr}_2\}$ linking units due to dense packing. Identical orientation of the chains is observed in neighboring layers. Colour scheme: V: teal, Sr: bright green, O: red, N: blue, C: light grey; H atoms are omitted for clarity.

The crystal lattice of **2** is formed by Sr-linked $\{\text{V}_{10}\}$ units *via* V-O-Sr bonds. The $\{\text{V}_{10}\}$ cluster forms four coordinative bonds to two Sr^{2+} cations through the terminal oxygen ligands on top and at the bottom of the cluster. Each Sr center interacts with adjacent $\{\text{Sr}_2\text{V}_{10}\}$

units, forming two additional coordinative bonds with a μ -oxo ligand and a terminal oxo ligand (Fig. 2, top). Further stabilization of the alkaline earth metal centers is provided by the carbonyl groups of four DMF molecules resulting in an eight-coordinate, square antiprismatic coordination environment. The non-polar methyl groups of DMF point away from the chain assembly. The distance between neighboring strontium centers is *ca.* 4.20 \AA . Direct linkage of the $\{\text{V}_{10}\}$ units by the Sr centers results in short intra-chain distances of approximately 10.4 \AA between $\{\text{V}_{10}\}$ units, see Fig. 2, middle.

The crystal packing reveals that the chains assemble parallel to each other with the same direction of propagation within one layer of the crystal. The 1D chains are aligned so that bridging $\{\text{Sr}_2\}$ units are located next to the $\{\text{V}_{10}\}$ units of adjacent chains. This behavior is due to the larger diameter of $\{\text{Sr}_2\}$ (maximum dimensions *ca.* 16 \AA \times *ca.* 11 \AA), so that these units act like a “molecular zipper”, slotting into place and giving an alternating pattern of bridging unit and cluster unit. Neighboring layers show an identical arrangement; however, due to the space requirement of the $\{\text{Sr}_2\}$ bridging units, a horizontal shift between neighboring layers is observed, see Fig. 2, bottom.

Mass-spectrometric studies

The solution and gas phase stability as well as the assembly and disassembly mechanisms of **1** and **2** were investigated using electrospray ionization mass-spectrometry (ESI-MS).¹⁷⁻²¹ For the analysis, a *ca.* $2.5 \cdot 10^{-4} \text{ M}$ solution of **1** in DMF was prepared. Analysis of the data reveals that the chains in **1** disassemble and a number of $\{\text{V}_{10}\}$ -based species are detected in region $< 500 \text{ m/z}$. The most prominent signals are species such as $[\text{H}_4\text{V}_{10}\text{O}_{28}]^{2-}$, $[\text{V}_{10}\text{O}_{26}]^{2-}$ and smaller fragments e.g. $[\text{V}_6\text{O}_{16}]^{2-}$. Furthermore reduced cluster fragments e.g. $[\text{V}^{\text{V}}_8\text{V}^{\text{IV}}\text{O}_{23}]^{2-}$ and $[\text{V}^{\text{V}}_8\text{V}^{\text{IV}}\text{O}_{25}]^{2-}$ were detected. It is suggested that reduction is due to the ESI-MS conditions. Notably, no chain fragments containing strontium or larger poly-cluster assemblies were detected in the higher m/z range.

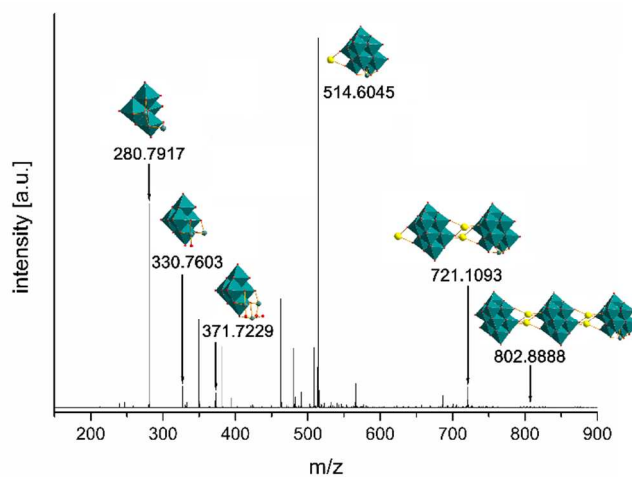


Fig. 3: ESI-MS analysis of **2** in the m/z range from 200 – 900. Peak assignment along with the proposed cluster fragments is shown. Structural presentation of cluster fragments is for illustration purposes only. Colour scheme: V/ $[\text{VO}_6]$: teal, Sr: yellow, O: red.

ESI-MS analysis of a methanolic solution of **2** (ca. $2.5 \cdot 10^{-4}$ M) reveals that **2** also shows disassembly of the principal $\{V_{10}\}$ building block in lower m/z region, giving cluster fragments such as $[HV_4O_{11}]^-$ and $[V_{10}O_{26}]^{2-}$. Typically, these fragments feature missing oxo ligands. In higher m/z regions, $\{V_{10}\}$ fragments containing strontium, e.g. $[SrV_{10}O_{27}]^{2-}$ were identified (see SI). Furthermore, larger poly-cluster assemblies with intact $\{V_{10}\}$ units linked by Sr^{2+} were observed. The largest species assigned features three decavanadate units with two intact Sr-based bridging units $\{H_2[SrV_{10}O_{27}][Sr_2V_{10}O_{28}][Sr_2V_{10}O_{28}]\}^{4-}$ observed at $m/z = 824.3614$ (calcd: 824.3609). Notably, the species observed do not feature stabilizing DMF ligands.

Conclusions

In conclusion, we show an easy control mechanism which allows the precise arrangement of infinite 1D strontium vanadium oxide chains in the solid state. The crystal engineering approach allowed us to link decavanadate clusters by dinuclear, urea-bridged strontium moieties; alternatively, direct linkage by strontium cations without the use of additional organic bridging ligands was achieved. Both vanadium oxide chains were formed *via* self-assembly from molecular precursors in straight-forward syntheses. The results show how small organic ligands such as urea can serve as structure directing groups, allowing the precise variation of the intra-chain cluster spacing. Mass-spectrometric studies give initial insight into the chain fragments present in solution and also provide a first glimpse at the initial stages of crystallization.

Future work will be required to further establish the exact role of urea and to determine whether it can be employed in a more general sense as structure-directing agent for polyoxometalate aggregates. In addition, the selective conversion of 1D chains into 2D grids or 3D frameworks by the introduction of cross-linking ligands. Furthermore deposition of the chains on surfaces to allow nanostructuring will be studied.

Experimental

General remarks

Synthetic and analytical details for **1** and **2** are given in the ESI. All chemicals were used as purchased without further purification. $(^nBu_4N)_3[H_3V_{10}O_{28}]$ was prepared according to published procedures.¹²

Synthesis of $\{[Sr(dmff)_3(CON_2H_4)_2][Sr(dmff)_2(CON_2H_4)_2][V_{10}O_{28}]\}$ (**1**):

$(^nBu_4N)_3[H_3V_{10}O_{28}]$ (0.20 g, 0.12 mmol, 1 eq.), $SrBr_2 \cdot 6 H_2O$ (0.09 g, 0.25 mmol, 2.08 eq.) and CON_2H_4 (0.06 g, 1.07 mmol, 8.92 eq.) were suspended in *N,N*-dimethyl formamide (DMF, 6 ml) and the reaction mixture was heated to 70 °C for 2 h. The color changed from orange to reddish orange and H_2O (200 μ l) was added. Diffusion crystallization with acetone as diffusion solvent resulted in yellow crystalline plates. The crude product was washed with acetone and was air-dried. Yield: 10.2 mg (5.87 μ mol, 4.89 % based

on V). Elemental analysis for $Sr_2V_{10}O_{37}C_{19}N_{13}H_{51}$ in wt% (calcd.): C 12.83 (13.11), N 10.26 (10.47), H 2.96 (2.96).

Synthesis of $\{[Sr(dmff)_4][V_{10}O_{28}]\}$ (**2**):

$(^nBu_4N)_3[H_3V_{10}O_{28}]$ (0.409 g, 0.24 mmol, 1 eq.) and $SrBr_2 \cdot 6 H_2O$ (0.173 g, 0.49 mmol, 2.04 eq.) were dissolved in DMF (5 ml). After the addition of H_2O (400 μ l) the orange solution was heated to 70 °C for 2 h. Diffusion crystallization with acetone as diffusion solvent yielded orange single crystalline blocks. The crude product was washed with acetone and was air-dried. Yield: 155.1 mg (0.09 mmol, 75 % based on V). Elemental analysis for $Sr_2V_{10}O_{36}C_{24}N_8H_{56}$ in wt% (calcd.): C 16.83 (16.77), N 6.08 (6.52), H 3.42 (3.29).

Crystallography of **1** and **2**

Single-crystal structure determination. Suitable single crystals of the respective compound were grown and mounted onto a microloop using Fomblin oil. X-ray diffraction intensity data were measured at 150 K on a Nonius Kappa CCD diffractometer ($\lambda(MoK\alpha) = 0.71073$ Å) equipped with a graphite monochromator. Structure solution and refinement was carried out using SHELX-2013 package through OLEX2. Corrections for incident and diffracted beam absorption effects were applied using empirical methods. Structures were solved by a combination of direct methods and difference Fourier syntheses and refined against F^2 by the full matrix least-squares technique. Crystallographic data (1027674-1027675) can be obtained free of charge via www.ccdc.cam.ac.uk/conts/retrieving.html or from the Cambridge Crystallographic Data Center 12, Union Road, Cambridge CB2 1EZ; fax: (+44)-1223-336-033; or deposit@ccdc.cam

Acknowledgements

CS gratefully acknowledges the *Fonds der Chemischen Industrie* for a Liebig Fellowship. The *Deutsche Forschungsgemeinschaft DFG* (contract no STR1164/4-1), Ulm University and Friedrich-Alexander-University Erlangen-Nuremberg are gratefully acknowledged for financial support. Prof. Dr. Karsten Meyer (UV/Vis), Oliver Tröppner, Maximilian Dürr and Prof. Dr. Ivana Ivanovic-Burmazovic (ESI-MS), Prof. Dr. Dirk M. Guldi (IR) are acknowledged for access to analytical instruments.

Notes and references

^a Institute of Inorganic Chemistry I, Ulm University, Albert-Einstein-Allee 11, 89081 Ulm, Germany. E-mail: carsten.streb@uni-ulm.de; Fax: +49-731-5023039; Tel: +49-731-5023867

Electronic Supplementary Information (ESI) available: synthetic, analytical and crystallographic details are given. See DOI: 10.1039/b000000x/

1. M. T. Pope, Y. Jeannin and M. Fournier, *Heteropoly and isopoly oxometalates*, Springer-Verlag Berlin, 1983.
2. M. T. Pope and A. Müller, *Angew. Chem. Int. Ed.*, 1991, **30**, 34.
3. Special POM issue: C. L. Hill (guest ed.), *Chem. Rev.*, 1998, **98**, 1.
4. POM-themed issue: L. Cronin and A. Müller (guest eds.), *Chem Soc Rev*, 2012, **41**, 7325.

Journal Name

5. D. L. Long, R. Tsunashima and L. Cronin, *Angew. Chem. Int. Ed.*, 2010, **49**, 1736.
6. C. L. Hill, *Compreh. Coord. Chem. II*, 2003, **4**, 679.
7. POM-special issue: U. Kortz and T. Liu (guest eds.), *Eur. J. Inorg. Chem.*, 2013, **2013**, 1556.
8. H. Abbas, A. L. Pickering, D. L. Long, P. Kögerler and L. Cronin, *Chem. Eur. J.*, 2005, **11**, 1071.
9. Y. Wang, S. L. Pan, H. W. Yu, X. Su, M. Zhang, F. F. Zhang and J. Han, *Chem. Commun.*, 2013, **49**, 306.
10. D. L. Long, E. Burkholder and L. Cronin, *Chem. Soc. Rev.*, 2007, **36**, 105.
11. V. Soghomonian, Q. Chen, R. C. Haushalter, J. Zubieta and C. J. Oconnor, *Science*, 1993, **259**, 1596.
12. C. Streb, R. Tsunashima, D. A. MacLaren, T. McGlone, T. Akutagawa, T. Nakamura, A. Scandurra, B. Pignataro, N. Gadegaard and L. Cronin, *Angew. Chem. Int. Ed.*, 2009, **48**, 6490.
13. K. Kastner and C. Streb, *CrystEngComm*, 2013, **15**, 4948.
14. K. Kastner, B. Puscher and C. Streb, *Chem. Commun.*, 2013.
15. T. Blasco, and J. M. Nieto. *Appl. Catal. A*: 1997, **157**, 117-142.
16. S. Kobayashi, N. Hamasaki, M. Suzuki, M. Kimura, H. Shirai, and K. Hanabusa *J. Am. Chem. Soc.* 2002, **124**, 6550-6551.
17. D. L. Long, C. Streb, Y. F. Song, S. Mitchell and L. Cronin, *J. Am. Chem. Soc.*, 2008, **130**, 1830.
18. E. F. Wilson, H. Abbas, B. J. Duncombe, C. Streb, D. L. Long and L. Cronin, *J. Am. Chem. Soc.*, 2008, **130**, 13876.
19. L. Vila-Nadal, A. Rodriguez-Forteza, L. K. Yan, E. F. Wilson, L. Cronin and J. M. Poblet, *Angew. Chem. Int. Ed.*, 2009, **48**, 5452.
20. J. Yan, D. L. Long, E. F. Wilson and L. Cronin, *Angew. Chem. Int. Ed.*, 2009, **48**, 4376.
21. E. F. Wilson, H. N. Miras, M. H. Rosnes and L. Cronin, *Angew. Chem. Int. Ed.*, 2011, **50**, 3720.